Journal of Nuclear Medicine, published on May 30, 2019 as doi:10.2967/jnumed.118.224568

^{89}Zr-immuno-PET: towards a non-invasive clinical tool to measure target engagement of therapeutic antibodies in-vivo

Yvonne W.S. Jauw[1,2], Joseph A. O'Donoghue[3], Josée M. Zijlstra[1], Otto S. Hoekstra[2], C. Willemien Menke-van der Houven van Oordt[4], Franck Morschhauser[5], Jorge A. Carrasquillo[6,7], Sonja Zweegman[1], Neeta Pandit-Taskar[6,7], Adriaan A. Lammertsma[2], Guus. A.M.S. van Dongen[2], Ronald Boellaard[2], Wolfgang A. Weber[6,7], Marc C. Huisman[2]

Author's affiliations

[1] Amsterdam UMC, Vrije Universiteit Amsterdam, Department of Hematology, Cancer Center Amsterdam, Amsterdam, the Netherlands

[2] Amsterdam UMC, Vrije Universiteit Amsterdam, Department of Radiology & Nuclear Medicine, Cancer Center Amsterdam, Amsterdam, the Netherlands

[3] Department of Medical Physics, Memorial Sloan Kettering Cancer Center, New York, USA

[4] Amsterdam UMC, Vrije Universiteit Amsterdam, Department of Medical Oncology, Cancer Center Amsterdam, Amsterdam, the Netherlands

[5] Univ. Lille, EA7365-GRITA-Groupe de Recherche sur les forms Injectables et les Technologies Associées; CHU Lille, Department of Hematology; F-59000 Lille, France

[6] Department of Radiology, Memorial Sloan Kettering Cancer Center, New York, USA

[7] Molecular Imaging and Therapy Service, Memorial Sloan Kettering Cancer Center, New York, USA

First/corresponding author

Yvonne Jauw

De Boelelaan 1117, 1081 HV Amsterdam, The Netherlands

Phone:+31204442604/Fax:+31204442601

Email: yws.jauw@vumc.nl

Potential conflicts of interest

WAW: Research support: Ipsen, Piramal, BMS, Blue Earth Diagnostics. Advisor: Advanced Accelerator applications, Bayer, Blue Earth Diagnostics, Ipsen, Endocyte, Piramal, Progenics. No other potential conflicts of interest relevant to this article exist.

Financial support

This research was financially supported by the Dutch Cancer Society (grant VU2013-5839 to YJ) and the Cancer Center Amsterdam (travel grant to YJ).

Word count: 4998

Running title: Zr-mAb-PET to measure target engagement

ABSTRACT

Rationale

Zirconium-89-immuno-positron emission tomography (^{89}Zr-immuno-PET) is a promising non-invasive clinical tool to measure target engagement of monoclonal antibodies (mAbs); in normal tissues to predict toxicity and in tumors to predict efficacy. Quantification of ^{89}Zr-immuno-PET will need to move beyond standardized uptake values (SUV), since total uptake may contain a significant non-target-specific contribution. Non-specific uptake is reversible (e.g. blood volume) or irreversible (due to ^{89}Zr-residualization after mAb degradation). The aim of this study was to assess non-specific uptake in normal tissues as a first critical step towards quantification of target engagement in normal tissues and tumors using ^{89}Zr-immuno-PET.

Methods

Data from clinical studies with 4 ^{89}Zr-labeled intact IgG1 antibodies were collected, resulting in a total of 128 PET scans (1 to 7 days p.i. from 36 patients: ^{89}Zr-antiCD20 (n=9), ^{89}Zr-antiEGFR (n=7), ^{89}Zr-antiPSMA (n=10) and ^{89}Zr-HER2 (n=10). Non-specific uptake was defined as uptake measured in tissues without known target expression. Patlak graphical evaluation of transfer constants was used to estimate the reversible (V_t) and irreversible (K_i) contributions to the total measured uptake for the kidney, liver, lung and spleen. Baseline values were calculated per tissue combining all mAbs without target expression (kidney: ^{89}Zr-antiCD20, ^{89}Zr-antiEGFR, ^{89}Zr-antiHER2; liver: ^{89}Zr-antiCD20; lung: ^{89}Zr-antiCD20, ^{89}Zr-antiEGFR, ^{89}Zr-antiPSMA; spleen: ^{89}Zr-antiEGFR, ^{89}Zr-antiHER2).

Results

Baseline V_t for the kidney, liver, lung and spleen was 0.20, 0.24, 0.09 and 0.24 mL·cm^{-3}, respectively. Baseline K_i was 0.7, 1.1, 0.2 and 0.5 µL·g^{-1}·h^{-1} for the kidney, liver, lung and spleen. For ^{89}Zr-antiPSMA, a four-fold higher K_i was observed for the kidney, indicating target engagement. In this case, non-specific uptake accounted for 66, 34 and 22% of the total signal in the kidney at 1, 3, 7 days p.i. respectively.

Conclusion

This study shows that non-specific uptake of mAbs for tissues without target expression can be quantified using ^{89}Zr-immuno-PET at multiple time points. These results form a crucial base for measurement of target-engagement by therapeutic antibodies *in-vivo* with ^{89}Zr-immuno-PET. For future studies, a pilot phase including at least 3 scans ≥

1 day p.i., is required to assess non-specific uptake as a function of time, to optimize study design for detection of target engagement.

Keywords:

Immuno-PET, Monoclonal antibodies, Zirconium-89, Molecular imaging, positron-emission tomography

INTRODUCTION

In-vivo assessment of target engagement is of interest to understand efficacy (tumor selectivity) and toxicity (due to target expression in normal tissues) of treatment with monoclonal antibodies (mAbs) or mAb conjugates. Currently, only plasma concentrations of mAbs can be easily measured in-vivo by obtaining blood samples. Direct measurement in tissues is difficult, as this requires invasive tissue sampling, limiting clinical application.

^{89}Zr-immuno-PET is a non-invasive, whole body technique with the potential to measure target engagement of therapeutic antibodies (or mAb conjugates) *in-vivo* (*1*). Future applications of this clinical tool are selection of mAbs during drug development and selection of patients who are likely to benefit from treatment (*2*).

Currently, it is common practice to report a single uptake value, expressed as standardized uptake value (SUV) or percentage injected activity per mL (%IA/mL) for ^{89}Zr-immuno-PET. However, the measured uptake in tissue is the sum of specific uptake (target engagement by the therapeutic antibody) and non-specific uptake (i.e. activity in the blood vessels or in the interstitial space that does not interact with the target and therefore has no pharmacologic effects). The ratio between specific uptake and non-specific uptake is expected to be time dependent. Measured uptake at early time points mainly consists of the blood volume fraction, while specific uptake increases over time. If specific uptake dominates, a single uptake value is an appropriate estimate to assess target engagement (*3*). This measurement is then expected to correlate with target expression in biopsies (determined by immunohistochemistry) and treatment outcome. However, also biopsy sampling has several limitations, e.g. sampling error and heterogeneity in target expression. Although biopsies may not provide a true gold standard for target engagement, it is the commonly available comparator. So far, clinical ^{89}Zr-immuno-PET studies have reported equivocal results; sometimes suggesting a correlation and sometimes not (*4-7*). These results indicate that a single uptake value could be insufficient due to the contribution of non-specific uptake. Therefore, knowledge of non-specific uptake is required to optimize study design.

The aim of this study was to assess non-specific uptake for tissues without target expression, as a first step towards quantification of target engagement using ^{89}Zr-immuno-PET.

Non-specific uptake is due to the blood volume fraction of the tissue, as well as antibody distribution (entering the tissue interstitium through paracellular pores, and through endothelial cells mediated by the neonatal Fc-receptor, leaving the tissue by convective transport through lymph flow) (Fig.1A)(*8*). At equilibrium, this

physiological component is linear with the plasma concentration (*9*) and is characterized as reversible uptake. In addition, non-specific catabolism of antibodies occurs by pinocytosis (e.g. in endothelial cells) and subsequent lysosomal proteolytic degradation (*10,11*). After the antibody is degraded, ^{89}Zr residualizes, leading to another component of non-specific uptake (Fig.1B)(*11,12,13*). This component is proportional to the area under the plasma time activity curve from the time of injection up to the scan time point, and is characterized as irreversible uptake. For tissues without target expression, this uptake is solely due to residualization of ^{89}Zr after non-target-mediated degradation of the mAb.

These two components of non-specific uptake can be quantified using graphical evaluation of transfer constants, commonly known as the 'Patlak linearization' approach as used for ^{18}F-FDG-PET (*14*). For tissues without target expression, we expect transfer constants in agreement with known literature for non-binding mAbs. For tissues with target expression, transfer constants would potentially differ due to target engagement (Fig.1C)(*15*).

MATERIALS AND METHODS

Data Collection

^{89}Zr-immuno PET scans and blood sample data were obtained for ^{89}Zr-obinutuzumab (*16*), ^{89}Zr-cetuximab (*17*), ^{89}Zr-huJ591 (*18*) and ^{89}Zr-trastuzumab (*19*)(Table 1). In the remainder of this report, the ^{89}Zr-labeled-mAbs used in these studies will be denoted as ^{89}Zr-antiCD20, ^{89}Zr-antiEGFR, ^{89}Zr-antiPSMA and ^{89}Zr-antiHER2, respectively. Data were selected based on the availability of scans at multiple time points (at least 3) for each patient, including plasma or serum activity concentrations from venous blood sampled at each scan time point.

Data was collected from 1) Amsterdam UMC, the Netherlands, 2) CHU Lille, France and 3) Memorial Sloan Kettering Cancer Center (MSKCC), USA. All studies were approved by an institutional review board and ethics committee. At CHU Lille and MSKCC, PET scans were acquired on a GE Discovery PET/CT scanner (GE Healthcare, Waukesha, WI, USA). At Amsterdam UMC, PET scans were acquired on a Philips Gemini TF-64 or Ingenuity TF-128 PET/CT scanner (Philips Healthcare, Best, the Netherlands). For all procedures, a low dose computed tomography scan was used for attenuation and scatter correction. Volumes of interest (VOI) of the kidney, liver, lung and spleen

were manually delineated on each scan and characterized by the mean radioactivity concentration in Bq·cm^{-3}. All radioactivity concentrations were decay corrected to the time of injection.

For each antibody, the Human Protein Atlas (*20*) was used as reference for lack of target antigen expression in tissues of interest.

Patlak Linearization

Patlak linearization applied to multiple-time tissue activity concentration measurements allows an estimate of the reversible and the irreversible contributions to the measured activity. The method was initially applied to blood-to-brain transfer and considered the fate of a test solute to obtain transfer constants (*14,21*). For ^{89}Zr-immuno-PET, we utilized this method to determine reversible and irreversible non-specific uptake of therapeutic antibodies. This analysis was performed per patient, for each tissue (liver, spleen, lung, kidney).

Input data consisted of the activity concentration in plasma (AC_p in Bq·mL^{-1}) and in tissue (AC_t in Bq·cm^{-3}) as a function of time post injection. The data were plotted as

$$\frac{AC_t}{AC_p} = K_i \frac{\int_0^t AC_p(\tau)d\tau}{AC_p} + V_T,$$

with AC_t/AC_p along the y-axis and $\int AC_p(\tau)\mathrm{d}\tau / AC_p$ along the x-axis (commonly known as a 'Patlak plot').

The $\int AC_p(\tau)\mathrm{d}\tau$ term represents the area under the plasma curve from the time of injection up to the time of the measurement, and will be referred to as $AUC_p^{0\text{-}t}$. The offset of the Patlak plot represents the distribution volume V_T (in mL·cm^{-3}) and the slope of the Patlak plot, *Ki* (in mL·g^{-1}·min^{-1}), the net rate of irreversible uptake.

Late time points (defined as ≥ 1day p.i) were included in the linear fit, as equilibrium state was assumed for these time points (*1*). Early time points (scans at 1h p.i.) were therefore not included.

The quality of the linear fit was assessed if at least 3 late time points were available. An r-value>0.9 was considered acceptable. Linear fits with an r-value <0.9 were excluded from the analysis.

The reversible and irreversible contributions to the uptake of ^{89}Zr-mAb (AC^f) at each time point were calculated as

$$AC_t^r = V_T \cdot AC_p, and\ AC_t^i = K_i \cdot AUC_p^{0-t},$$

with superscript *r* for the reversible and *i* for the irreversible component. In addition, the percentage difference between fitted ($AC^f = AC^r + AC^i$) and measured tissue activity concentrations per time point was calculated as (AC^f-AC^t)/AC^t x 100 (%).

Predicted Values for Transfer Constants

The transfer constants obtained were interpreted in terms of physiological components of antibody biodistribution. A literature search was performed to obtain predicted values for these physiological components for a non-binding intact IgG1 mAb.

To predict the value for the reversible component for a non-binding mAb, we used the proportionality constant between the tissue and plasma concentration, referred to as the antibody biodistribution coefficient (ABC). ABC for various tissues were obtained by a physiologically-based pharmacokinetic (PBPK) model of mAbs and validated with experimental data (*9*). The reported ABC for brain was 0.004 (*9*), indicating that the plasma volume fraction of 0.02 (*22*) was not included. Therefore, we defined the predicted value for V_T as the ABC plus the plasma volume fraction (within a 2-fold error margin, as reported for all ABC). The volume fraction was calculated as the plasma volume of the tissue (in mL) divided by the total volume of the tissue (in mL). Plasma and total tissue volumes were obtained from previously published physiological model parameters for human (*22*). For example, for the kidney, the reported ABC was 0.137 and the plasma volume fraction 0.055 (*22*), leading to a predicted V_T of 0.19. The predicted values for V_T for liver and spleen were 0.21 and 0.25 (*9,22*). The ABC for lung requires special consideration, since lung has a density of ~0.3g/mL. Volumes of distribution are in $mL \cdot cm^{-3}$, and therefore the ABC for lung was divided by three in order to compare with V_T values derived from ^{89}Zr-immuno-PET. For lung, the predicted value for V_T was 0.10 (*9,22*).

For tissues without target expression, the entire irreversible component is due to non-target mediated mAb degradation (and subsequent residualizing of ^{89}Zr). Endosomal mAb degradation is a non-specific catabolic mechanism for all intact IgG molecules. Per day, 6.3% of the intravascular IgG pool is catabolized (*23*). Therefore, the whole body catabolic rate was estimated at 7.8 $mL \cdot h^{-1}$, using a reference total plasma volume (22). The contribution of individual tissues (experimentally determined in mice) was 6%, 30%, 1.3% and 2.8% for kidney,

liver, lung and spleen, respectively (*11*). These values were used to predict the irreversible component for tissues without target expression.

To compare the ^{89}Zr-immuno-PET derived value for the net rate of irreversible uptake in $\mu L \cdot g^{-1} \cdot h^{-1}$ to the catabolic rate in $mL \cdot h^{-1}$, K_i was multiplied by tissue volume (*22*).

Predicted values for V_T and K_i, including literature values used, are presented in Supplemental Table 1.

Statistical Analysis

Values for V_T and K_i are presented per tissue, and per ^{89}Zr-mAb. Median values and interquartile ranges were reported due to the small sample size per group.

In addition, a baseline value was obtained by combining the *n* values for tissues without target expression. For example, no target expression in the kidney was reported for CD20, EGFR and HER2 (Table 1) (*20*). Therefore, ^{89}Zr-antiCD20, ^{89}Zr-antiEGFR and ^{89}Zr-antiHER data were combined to determine the baseline value for V_T and K_i, for kidney tissue without target expression. Baseline values for liver consisted of ^{89}Zr-antiCD20. For lung, data on ^{89}Zr-antiCD20, ^{89}Zr-antiEGFR and ^{89}Zr-antiPSMA were combined to obtain the baseline value. For spleen, the baseline value consisted of ^{89}Zr-antiEGFR and ^{89}Zr-antiHER2.

The Wilcoxon signed rank test was used to determine whether the *n* values for V_T for tissues without target expression (baseline values) differed from the predicted value. A p-value <0.05 was considered statistically significant. Statistical tests were performed in GraphPad Prism, version 6.02.

RESULTS

Patlak Linearization

Per patient, Patlak linearization was conducted for each tissue (kidney, liver, lung, spleen) (Fig.2). An r-value of >0.9 was obtained for 71/80 linear fits for ^{89}Zr-antiPSMA and ^{89}Zr-antiHER2 (3 late time points available). Therefore, we assumed that data for ^{89}Zr-antiCD20 and ^{89}Zr-EGFR were consistent with the assumptions under the Patlak method. For these datasets, the r-value for the linear fit could not be obtained (only 2 late time points available). For ^{89}Zr-antiHER2 an *r*-value <0.9 was obtained for 1/10 fits for kidney uptake, 2/10 for liver, 4/10 for lung and 2/10 for

spleen. The mean percentage difference between fitted and measured tissue activity concentrations per time point for all fits through 3 time points with r >0.9 was ±4%, except for ^{89}Zr-antiPSMA in the kidney (Supplemental Table 2).

Volume of Distribution (V_T)

Values for V_T per mAb are presented in Table 2. Non-specific, reversible uptake is reflected by baseline values for V_T for tissues without target expression. For the kidney, liver, lung and spleen respectively, measured baseline values for V_T were 0.20 (0.16-0.25), 0.24 (0.21-0.28), 0.09 (0.07-0.10) and 0.24 (0.20-0.27) mL·cm^{-3}. For these tissues, the predicted values for V_T (ABC + plasma volume fraction) were 0.19, 0.21, 0.10 and 0.25, respectively. No differences were observed between the measured baseline value for V_T and the predicted value for kidney (p=0.24; *n*=25), liver (p= 0.07; *n*=9) and spleen (p=0.12; *n*=15). For lung, the measured baseline value for V_T (0.09, 0.07-0.10) was statistically different (p< 0.02; *n*=25) from the predicted value of 0.10, but within the two-fold error range (0.05-0.20) of the predicted value.

Net Rate of Irreversible uptake (K_i)

Values for K_i per mAb are presented in Table 3. Non-specific, irreversible uptake is reflected by baseline values for K_i for tissues without target expression. For kidney, liver, lung and spleen respectively, measured baseline values for K_i were 0.7 (0.4-1.3), 1.1 (0.8-2.1), 0.2 (0.1-0.3) and 0.5 (0.3-0.7) µL·g^{-1}·h^{-1}. For kidney, the baseline catabolic rate was 0.23 mL·h^{-1}, equal to 3% of the whole body catabolic rate (predicted value 6%). Fractional catabolic rate of liver, lung and spleen were 30%, 3% and 1%, respectively (predicted values were 30%, 1.3% and 2.8%).

Detection of Target Engagement

In case of target engagement (Fig.1C), we expect to observe an increased rate of irreversible uptake compared to the baseline value. Expression of PSMA was reported for the kidney (*18*) and therefore target engagement of ^{89}Zr-antiPSMA is expected in this tissue. Patlak linearization for ^{89}Zr-antiPSMA was performed (Fig.3). In this case, a four-fold higher K_i (2.8 vs 0.7) was obtained compared to the baseline value for the kidney, indicating target engagement by irreversible uptake. For liver, an increased K_i was observed for ^{89}Zr-antiEGFR, ^{89}Zr-antiPSMA and ^{89}Zr-antiHER2

189 (3.8, 5.7 and 1.7 respectively compared to 1.1), corresponding with known target expression (*20*). No increased K_i

190 was observed for lung and spleen (Table 3).

DISCUSSION

^{89}Zr-immuno-PET is a promising, non-invasive clinical tool to measure antibody target engagement *in-vivo.* As a first step towards quantification of target engagement, non-specific uptake for tissues without target expression was assessed for four ^{89}Zr-labeled mAbs. This study showed that non-specific, reversible uptake (V_T) was similar to the predicted value for a non-binding mAb. Non-specific, irreversible uptake (K_i) corresponded with the predicted value for the fractional catabolic rate of IgG. Patlak linearization is applied to data obtained from a single subject. The range of values observed for the baseline transfer constants reflects inter-patient variability. This method allows, for a single subject, to assess whether target-mediated binding does occur in a certain normal tissue for the antibody under investigation. Similar as for PKPD type analysis, Patlak linearization can be applied with sparse temporal sampling, but does not require assumptions that underlying parameters are the same among patients. Moreover, it uses the individually measured input functions, i.e. bioavailability of the tracer in blood over time and it can therefore account for inter-individual variability of the tracer bioavailability in the central compartment (i.e. blood). For these reasons this method was applied in our present study. An increase in K_i indicates target engagement, as was observed for e.g. ^{89}Zr-antiPSMA in the kidney. In this study, baseline values for K_i and V_T were tissue dependent. Especially for the liver, relatively high non-specific, irreversible uptake was observed compared to other tissues, indicating that this organ is strongly involved in mAb catabolism. Therefore, detection of target engagement with a single uptake value is expected to be more difficult in the liver.

Study design can have a significant impact of the ability to detect target engagement. For example, for ^{89}Zr-antiCD20, no increase of irreversible uptake (K_i) was observed in the spleen, although expression of CD20 in the spleen is known to be high (*20*). A plausible explanation for this observation is saturation of the CD20 receptors due to high dose of unlabeled antiCD20 (1000mg), which was administered before the radiolabeled antibody. So, antibody dose is a parameter to be taken into account in assessment of target engagement. Another important consideration for design of ^{89}Zr-immuno-PET studies, is that scans obtained at multiple late time points are required for the Patlak linearization to determine reversible and irreversible uptake. At least 3 late time points are required to assess whether the data can be fitted to a straight line.

In some cases (9/80), the data could not be described by a linear fit. Especially for the lung (4/9), this could be explained by a unfavorable signal to noise ratio (low signal and relative low tissue density). The observed overestimation of fitted uptake data at 24h p.i. accompanied with an underestimation of the uptake at 48-120h p.i. for ^{89}Zr-antiPSMA in the kidney only may indicate that the reversible uptake processes were not yet in the equilibrium state at 24h p.i.. From a methodological perspective, collection of more data points would be preferred. This method could be further validated in future preclinical ^{89}Zr-immuno-PET studies, where scans at more time points can be acquired, including invasive tissue sampling to assess target expression by immunohistochemistry.

Usually, ^{89}Zr-immuno-PET scans are analyzed at a single time point, representing the sum of all physiological components of antibody distribution, being either target specific or non-specific. This study showed how the various physiological components of antibody distribution contribute to the measured SUV (Figs.2 and 3). For the kidney as an example, a SUV of around 2.5 was measured for ^{89}Zr-antiPSMA at 1 to 7days p.i.. Non-specific uptake was estimated to account for a SUV of 1.6 (66%) at 1day p.i.. The contribution of non-specific uptake decreased to a SUV of 0.6 (22%) at 7days p.i..

Detection of target engagement in normal tissues is of interest to assess which mAb has potential for further development into an antibody-drug conjugate (ADC). For an ADC, absence of target engagement in normal tissues is considered important to limit potential toxicity.

To understand and predict efficacy of mAb-based treatments, measurement of target engagement in tumors is essential. However, the method described in this paper cannot be directly applied to tumors, as these are expected to be more complex than normal tissues. Non-specific, reversible uptake in tumors (blood volume fraction and non-target mediated antibody distribution to tumor tissue (“tight or leaky tissue”)) may be more variable between tumors and between patients. In addition, non-specific, irreversible uptake may be increased by the rate of protein catabolism in the tumor and uptake in tumor immune filtrates (e.g. macrophages). In future work, we aim to explore which method can be applied to measure target engagement for tumors. Especially target-negative tumors are of interest to study factors that influence non-specific uptake.

In the present study, ^{89}Zr-immuno-PET was used as a non-invasive clinical tool to assess physiological components of antibody distribution *in-vivo* and target engagement of therapeutic antibodies was observed. For

future studies to assess target engagement for other ^{89}Zr-labeled mAbs, a multiple time point pilot study (with at least 3 late time points) is advised to determine the contribution of non-specific uptake as a function of time and mAb dose. This knowledge can be used to optimize study design and assess whether single time point scanning to detect target engagement is feasible and at which time point.

This concept is widely applicable as mAbs and mAb conjugates against many target antigens are developed for a broad range of clinical indications.

CONCLUSION

This study shows that non-specific uptake of mAbs for tissues without target expression can be quantified using ^{89}Zr-immuno-PET at multiple time points. These results form a crucial base for measurement of target-engagement by therapeutic antibodies *in-vivo* with ^{89}Zr-immuno-PET. For future studies, a pilot phase including at least 3 scans at ≥ 1 day p.i., is required to assess non-specific uptake as a function of time, to optimize study design for detection of target engagement.

ACKNOWLEDGEMENTS

We thank Mats Bergstrom (independent external imaging consultant, Uppsala, Sweden) for conceptual support.

KEY POINTS

Question: Can we move quantification of ^{89}Zr-immuno-PET beyond SUV, since total uptake may contain a significant non-target specific contribution?

Pertinent Findings: In this retrospective analysis of clinical ^{89}Zr-immuno-PET studies, non-specific uptake was quantified in normal tissues without target expression. The magnitude of non-specific uptake in normal tissues was related to its physiological basis (i.e. blood volume, mAb biodistribution and ^{89}Zr-residualization after mAb degradation).

Implications for Patient Care: Non-specific uptake of ^{89}Zr-labeled mAbs in normal tissues can be quantified to optimize detection of target engagement of therapeutic antibodies in-vivo.

REFERENCES

1. Bergstrom M. The use of microdosing in the development of small organic and protein therapeutics. *J Nucl Med.* 2017;58:1188-1195.
2. Jauw YWS, Menke-van der Houven van Oordt CW, Hoekstra OS, et al. Immuno-positron emission tomography with zirconium-89-labeled monoclonal antibodies in oncology: what can we learn from initial clinical trials? *Front Pharmacol.* 2016;7:131.
3. Lammerstma AA. Forward to the past: the case for quantitative PET imaging. *J Nucl Med.* 2017;58:1019-1024.
4. Gaykema SB, Brouwers AH, Lub-de Hooge MN, et al. ^{89}Zr-bevacizumab PET imaging in primary breast cancer. *J Nucl Med.* 2013;54:1014–1018.
5. Lamberts TE, Menke-van der Houven van Oordt CW, Ter Weele EJ, et al. ImmunoPET with anti-mesothelin antibody in patients with pancreatic and ovarian cancer before anti-mesothelin antibody-drug conjugate treatment. *Clin Cancer Res.* 2016;22:1642–1652
6. Jauw YW, Zijlstra JM, de Jong D, et al. Performance of ^{89}Zr-labeled-rituximab-PET as an imaging biomarker to assess CD20 targeting: a pilot study in patients with relapsed/refractory diffuse large B cell lymphoma. *PLoS One.* 2017:12:e0169828.
7. McKnight BN, Viola-Villegas NT. ^{89}Zr-immunoPET companion diagnostics and their impact in clinical drug development. *J labelled Comp Radiopharm.* 2018;61:727-738.
8. Lobo ED, Hansen RJ, Balthasar JP. Antibody pharmacokinetics and pharmacodynamics. *J Pharm Sci.* 2004;93:2645-68.
9. Shah DK, Betts AM. Antibody biodistribution coefficients: inferring tissue concentrations of monoclonal antibodies based on the plasma concentrations in several preclinical species and human. *MAbs.* 2013;5:297-305.
10. Chen Y, Balthasar JP. Evaluation of a catenary PBPK model for predicting the in vivo disposition of mAbs engineered for high-affinity binding to FcRn. *AAPS J.* 2012;14:850-9.
11. Eigenmann MJ, Fronton L, Grimm HP, et al. Quantification of IgG monoclonal antibody clearance in tissues. *MAbs.* 2017;9:1007-1015.

12. Cheal SM, Punzalan B, Doran MG, et al. Pairwise comparison of 89Zr- and 124I-labeled cG250 based on positron emission tomography imaging and nonlinear immunokinetic modeling: in vivo carbonic anhydrase IX receptor binding and internalization in mouse xenografts of clear-cell renal cell carcinoma. *Eur J Nucl Med Mol Imaging.* 2014;41:985-94.
13. Ferl GZ, Kenanova V, Wu AM, DiStefano JJ. A two-tiered physiologically based model for dually labeled single-chain Fv-Fc antibody fragments. *Mol Cancer Ther.* 2006;5:1550-8.
14. Patlak CS, Blasberg RG, Fenstermacher JD. Graphical evaluation of blood-to-brain transfer constants form multiple-time uptake data. *J Cereb Blood Flow and Metab.* 1983;3):1-7.
15. Zhe L, Krippendorff BF, Sharma S, et al. Influence of molecular size on tissue distribution of antibody fragments. *MAbs.* 2016;8:113-119.
16. Jauw, Y, Zijlstra J, Hoekstra O, et al. First-in-human in-vivo biodistribution of a glyco-engineered antibody: ^{89}Zirconium-labeled obinutuzumab in patients with non-Hodgkin lymphoma. *J Nucl Med.* 2017: 58; supplement 1: 387.
17. Menke-van der Houven van Oordt, CW, Gootjes EC, Huisman MC, *et al.* ^{89}Zr-cetuximab PET imaging in patients with advanced colorectal cancer. *Oncotarget.* 2015;30:30384-93.
18. Pandit-Taskar N, O'Donoghue JA, Beylergil V, et al. ^{89}Zr-huJ591 immuno-PET imaging in patients with advanced metastatic prostate cancer. *Eur J Nucl Med Mol Imaging.* 2014;41:2093-2105.
19. O'Donoghue JA, Lewis JS, Pandit-Taskar N, et al. Pharmacokinetics, biodistribution, and radiation dosimetry for 89Zr-trastuzumab in patients with esophagogastric cancer. *J Nucl Med.* 2018; 59:161–166.
20. Uhlen M, Oksvold P, Fagerberg L, et al. Towards a knowledge-based Human Protein Atlas. *Nat Biotechnol.* 2010; 12:1248-50.
21. Blasberg RG, Fenstermacher JD, Patlak CS. Transport of α-aminoisobutyric acid across brain capillary and cellular membranes. *J Cereb Blood Flow and Metab.* 1983;3:8-32.
22. Shah DK, Betts AM. Towards a platform PBPK model to characterize the plasma and tissue disposition of monoclonal antibodies in preclinical species and human. *J. Pharmacokinet Pharmacodyn* 2012;39:67.
23. Waldmann TA, Strober W. Metabolism of immunoglobulins. *Prog Allergy.* 1969;13:1-110.

24. Weineisen K, Schottelius M, Simecek J. ^{68}Ga- and ^{177}Lu-labeled PSMA I&T: Optimization of a PSMA-targeted theranostic concept and first proof-of-concept human studies. *J Nucl Med.* 2015;56:1169-1176.

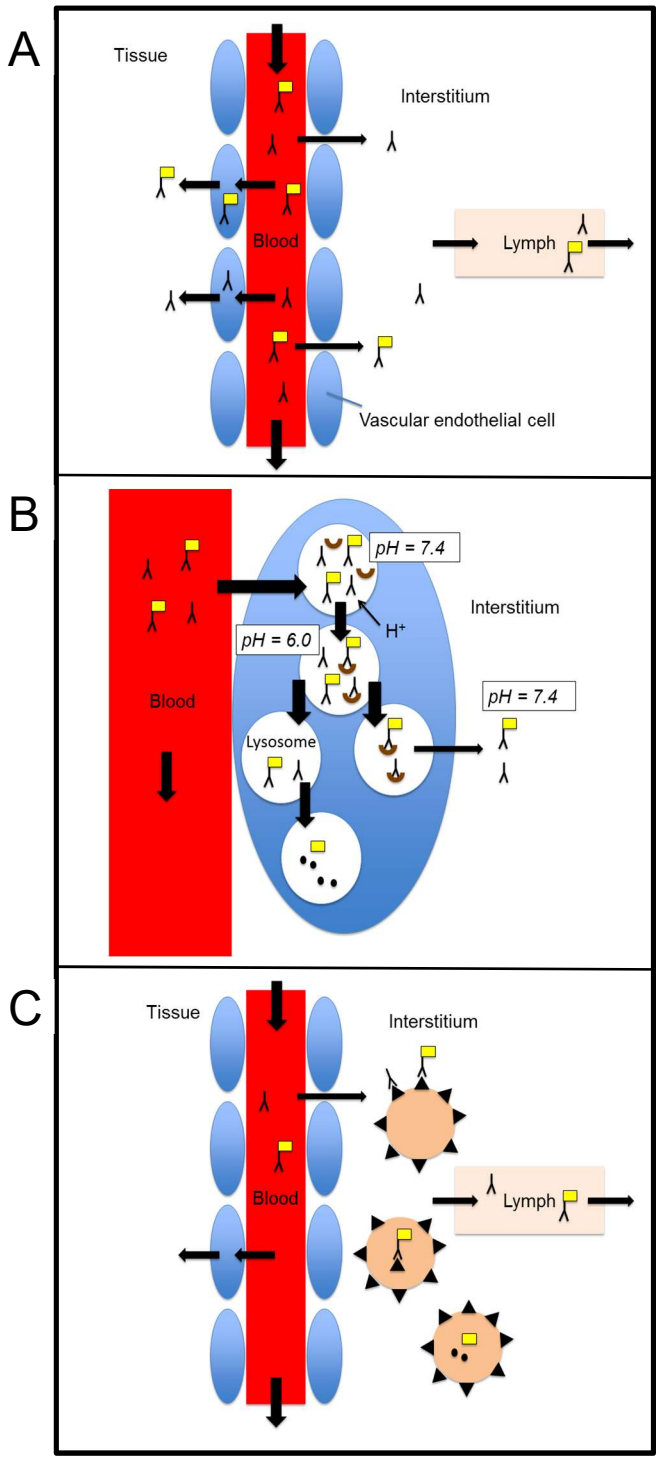

Figure 1 Biodistribution of a ^{89}Zr-labeled mAb: physiological components

Reversible non-specific uptake (A) due to antibody in the vascular tissue compartment and antibody entering the tissue interstitium through paracellular pores, and through endothelial cells mediated by the neonatal Fc-receptor, leaving the tissue by convective transport through lymph flow. Irreversible non-specific uptake (B) due to mAb degradation in the lysosome, followed by residualization of ^{89}Zr. Specific uptake (C) due to target engagement (target binding and internalization of mAb-target antigen).

Adapted from Lobo 2004 (8) and Chen 2012 (10).

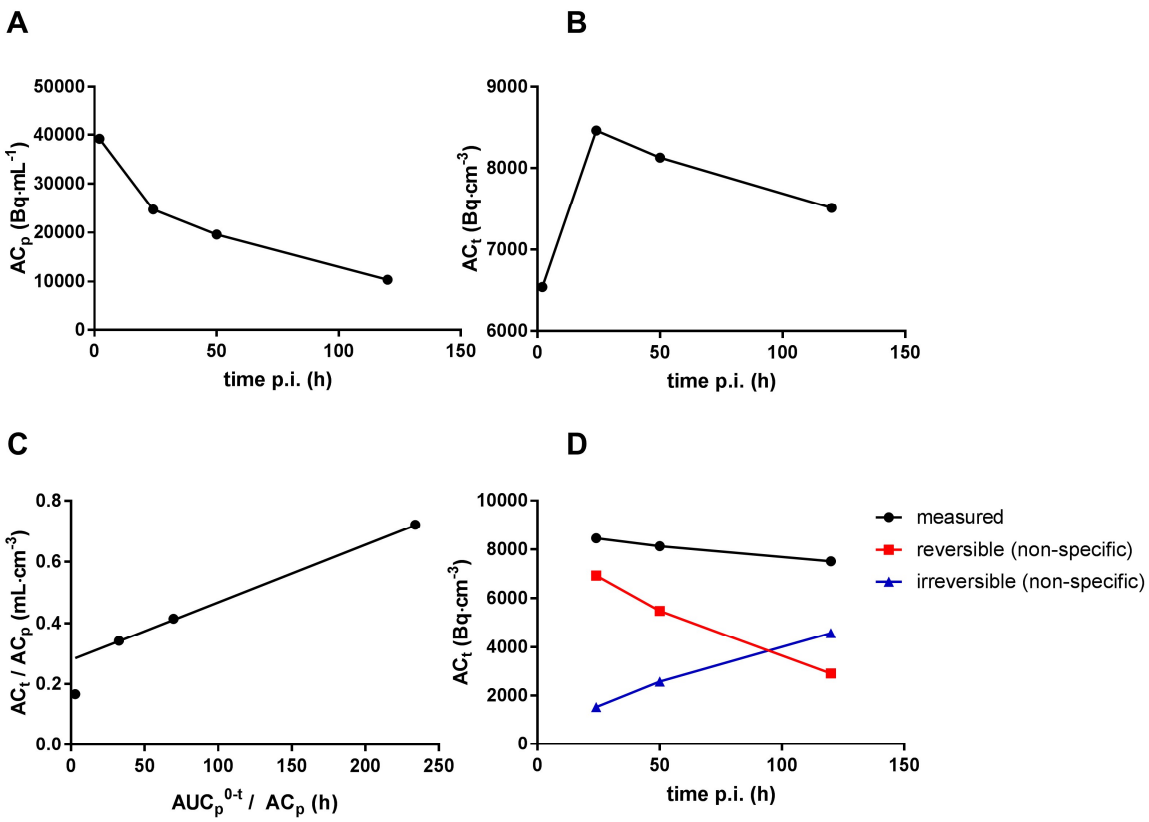

332

333 **Figure 2 Transfer constants for ^{89}Zr-antiHER2 in the kidney**

334 Example for one patient in the ^{89}Zr-antiHER2 study, with (A) measured activity concentrations in serum and (B)
335 measured activity concentrations in the kidney. Patlak linearization (C) to determine the offset (V_T) and slope (K_i) of
336 the linear fit to the last three time points (same data). (D) Reversible (red line) and irreversible (blue line)
337 contributions to the total measured signal (black line). No target expression has been reported for HER2 in the
338 normal kidney. Therefore, we hypothesize that the total signal consists of non-specific uptake. After 100h p.i., total
339 uptake predominantly consists of irreversible non-specific uptake due to ^{89}Zr-residualization after mAb
340 degradation.
341

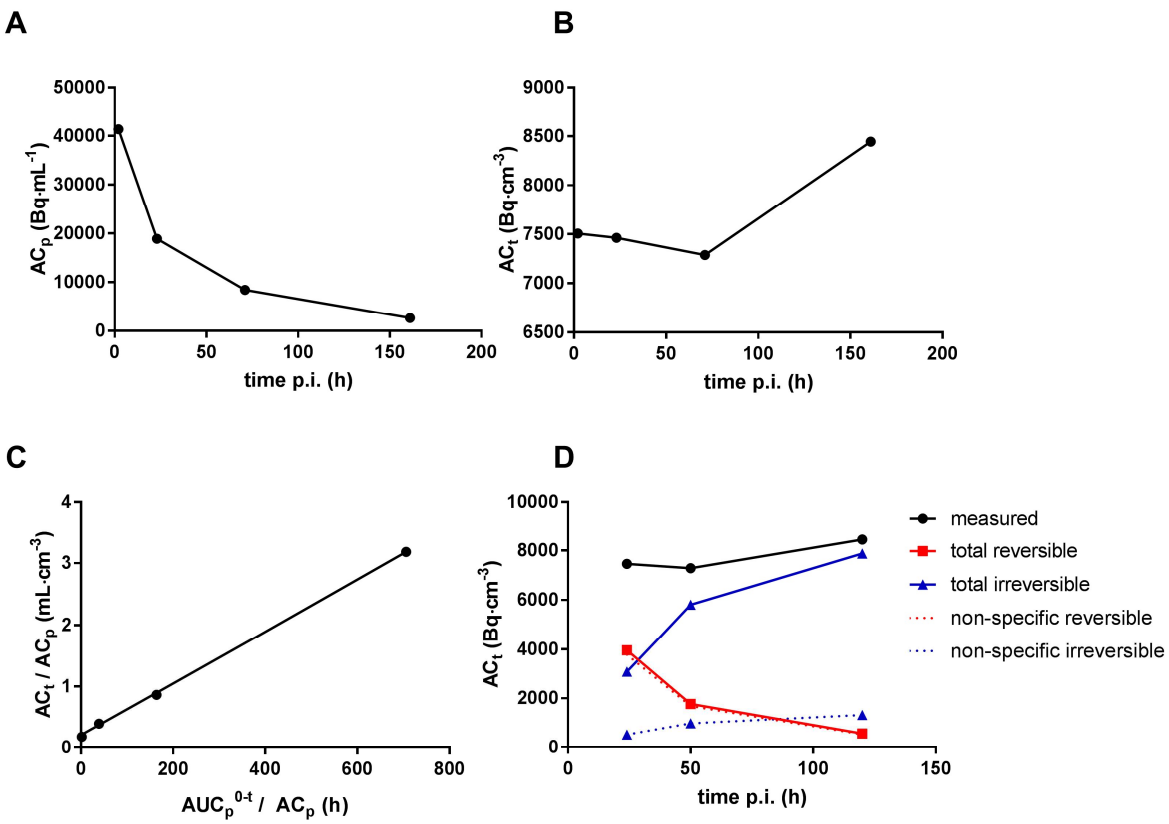

342

343 **Figure 3 Transfer constants for ^{89}Zr-antiPSMA in the kidney**

344 Example for one patient in the ^{89}Zr-antiPSMA study, with (A) measured activity concentrations in serum (*A*) and (B)
345 measured activity concentrations in the kidney. Patlak linearization (C) to determine the offset (V_T) and slope (K_i) of
346 the linear fit to the last three time points (same data). (D) Total reversible (red line) and total irreversible (blue line)
347 contributions to the measured signal (black line).
348 Dashed lines represent estimated values for non-specific reversible uptake (calculated as baseline $V_T \cdot AC_p$) and
349 non-specific irreversible uptake (calculated as baseline $K_i \cdot AUC_p^{0-t}$).
350 Non-specific uptake accounts for 66, 34 and 22% of the total measured signal at 1,3 and 7 days p.i., respectively.
351 The difference between total irreversible uptake (blue line) and estimated non-specific irreversible uptake (dashed
352 blue line) indicates target-mediated uptake.

353

Table 1 Data characteristics

	^{89}Zr-antiCD20	**^{89}Zr-antiEGFR**	**^{89}Zr-antiPSMA**	**^{89}Zr-antiHER2**
General information				
mAb	Obinutuzumab	Cetuximab	Hu-J591	Trastuzumab
Type	Humanized	Chimeric	Humanized	Humanized
IgG subclass	IgG1	IgG1	IgG1	IgG1
Target expression(*20*) - Kidney - Liver - Lung - Spleen	 Absent Absent Absent Present	 Absent Present Absent Absent	 Present Present Absent Absent*	 Absent Present Present Absent
Study design				
Center	Amsterdam UMC(n=4) CHU Lille(n=5)	Amsterdam UMC	MSKCC	MSKCC
Patient category	Non-Hodgkin lymphoma	Colo-rectal carcinoma	Prostate cancer	Gastric cancer
Number of patients	9	7	10	10
Injected activity/mAb dose	37MBq/10 mg 1000mg unlabeled mAb	37MBq/10mg 500mg/m^2 unlabeled mAb	185MBq/1.7mg total mass of 25mg mAb	185MBq/3mg total mass of 50mg mAb
Administration**	predose	predose	co-injection	co-injection
PET scan time points	1 hr,72h,144h p.i.	1hr,72h,144h p.i.	2-4h,24h,48-120h,144-168h p.i.	4h,24h,48-96h,120-192h p.i.
Blood sample***	plasma	plasma	serum	serum
Blood sampling timepoints	5,30,60,120min,24h****, 72h,144h p.i.	1-2h,24h,48h,72h,144h	5,30,60,120-240min,24h,48-120h, 144-168h p.i.	5,15,30,60min,2h,24h,48-96h, 120-192h p.i.
Reference	Jauw, et al.(*16*)	Menke, et al.(*17*)	Pandit-Taskar, et al.(*18*)	O'Donoghue,et al.(*19*)

*Expression of PSMA in the spleen has been reported(*24*)

**Administration: predose = ^{89}Zr-mAb within 2 hours after administration of unlabeled mAb.
co-injection = unlabeled mAb infused intravenously over 5min followed immediately by a 1min infusion of the radiolabeled mAb.

***Blood samples consisted of plasma or serum samples; assuming no practical difference between these assays for our purposes, since mAb binding does not occur to coagulation factors (the difference between plasma and serum).

****Blood samples obtained at 24h p.i. at CHU Lille(n=5), no 24h sample obtained at Amsterdam UMC

Table 2 Volume of distribution V_t

	^{89}Zr-antiCD20	^{89}Zr-antiEGFR	^{89}Zr-antiPSMA	^{89}Zr-antiHER2	Baseline
Kidney	0.18(0.15-020)	0.25(0.23-0.29)	0.28(0.21-0.32)	0.19(0.15-0.25)	0.20(0.16-0.25)
Liver	0.24(0.21-0.28)	0.64(0.54-0.91)	0.29(0.23-0.43)	0.24(0.22-0.29)	0.24(0.21-0.28)
Lung	0.08(0.08-0.10)	0.11(0.09-0.13)	0.07(0.06-0.09)	0.08(0.05-0.11)	0.09(0.07-0.10)
Spleen	0.20(0.18-0.21)	0.23(0.20-0.27)	0.22(0.20-0.28)	0.24(0.18-0.27)	0.24(0.20-0.27)

V_t (mL·cm^{-3}) presented as median (interquartile range)

Table 3 Net rate of irreversible uptake K_i

	^{89}Zr-antiCD20	^{89}Zr-antiEGFR	^{89}Zr-antiPSMA	^{89}Zr-antiHER2	Baseline
Kidney	0.4(0.2-0.6)	0.7(0.4-1.2)	2.8(2.4-3.1)	1.5(0.9-1.8)	0.7(0.4-1.3)
Liver	1.1(0.8-2.1)	3.8(1.9-5.8)	5.7(4.9-8.4)	1.7(1.4-2.0)	1.1(0.8-2.1)
Lung	0.2(0.1-0.3)	0.4(0.2-0.6)	0.1(0.0-0.2)	0.2(0.0-0.5)	0.2(0.1-0.3)
Spleen	0.6(0.5-0.8)	0.5(0.3-0.5)	1.5(1.2-1.7)	0.7(0.4-0.8)	0.5(0.3-0.7)

K_i ($\mu L \cdot g^{-1} \cdot h^{-1}$) presented as median (interquartile range)

Supplemental Table 1 Predicted and observed transfer constants

	Literature values						Predicted transfer constants		Observed transfer constants	
	ABC (2-fold error) (*9*)	total tissue volume (mL) (*22*)	tissue plasma volume (mL) (*22*)	plasma volume fraction *	Fraction of whole body catabolic rate per tissue (*11*)	No target expression for (*20*)	V_t †	K_i ‡	Baseline V_t §	Baseline K_i §
kidney	0.137 (0.07-0.27)	332	18.2	0.055	0.06	CD20 EGFR HER2	0.19	1.41	0.20 (0.16-0.25)	0.7 (0.4-1.3)
liver	0.121 (0.06-0.24)	2143	183	0.085	0.30	CD20	0.21	1.13	0.24 (0.21-0.28)	1.1 (0.8-2.1)
lung	0.149 ‖ (0.07-0.30)	1000	55	0.055	0.013	CD20 EGFR PSMA	0.10	0.10	0.09 (0.07-0.10)	0.2 (0.1-0.3)
spleen	0.128 (0.06-0.26)	221	26.8	0.121	0.028	EGFR HER2	0.25	0.99	0.24 (0.20-0.27)	0.5 (0.3-0.7)

Observed values for V_t ($mL \cdot cm^{-3}$) and K_i ($\mu L \cdot g^{-1} \cdot h^{-1}$) presented as median (interquartile range)

* Plasma volume divided by total tissue volume.

† ABC plus plasma volume fraction.

‡ Fraction of whole body catabolic rate per tissue multiplied by the estimated whole body catabolic rate of 7.8 $mL \cdot h^{-1}$, divided by the tissue plasma volume, multiplied by 1000.

§ To determine baseline values per tissue, data from ^{89}Zr-labeled mAbs, for which no target expression was reported, were used.

‖ The ABC for lung was reported as 0.149 based on quantified tissue biodistribution per gram. To correct for the density of the lung in the calculation of predicted Vt (per ml), the ABC was multiplied by 0.3 g/mL.

Supplemental Table 2 Relative difference between fitted and measured tissue activity concentrations

	^{89}Zr-antiHER2 24 h p.i.	^{89}Zr-antiHER2 48-96 h p.i.	^{89}Zr-antiHER2 120-192 h p.i.	^{89}Zr-antiPSMA 24 h p.i.	^{89}Zr-antiPSMA 48-120 h p.i.	^{89}Zr-antiPSMA 144-168 h p.i.
kidney	-1.1 (11.0) n=10	3.3 (14.3) n=10	-1.1 (3.6) n=10	18 .2 (14.5) n=9	-8.3 (6.6) n=9	2.0 (1.6) n=9
liver	3.5 (5.6) n=10	-3.3 (5.4) n=10	0.7 (2.1) n=10	0.5 (11.2) n=8	0.6 (6.2) n=8	0.1 (1.5) n=8
lung	-1.7 (6.1) n=10	3.0 (10.9) n=10	-0.6 (3.0) n=10	1.1 (5.0) n=6	-1.0 (10.4) n=6	0.0 (2.0) n=6
spleen	1.4 (4.0) n=10	-1.1 (4.9) n=10	0.2 (1.7) n=10	0.4 (8.2) n=8	0.2 (6.6) n=8	0.1 (1.4) n=8

Data presented as mean (SD) in %